Retention of immobile Se(0) in flow-through aquifer column systems during bioreduction and oxic-remobilization

Ho, Mallory S.

2022-08-15

Ho , M S , Vettese , G F , Morris , K , Lloyd , J R , Boothman , C , Bower , W R , Shaw , S & Law , G T W 2022 , ' Retention of immobile Se(0) in flow-through aquifer column systems during bioreduction and oxic-remobilization ' , Science of the Total Environment , vol. 834 , 155332 . https://doi.org/10.1016/j.scitotenv.2022.155332

http://hdl.handle.net/10138/355891
https://doi.org/10.1016/j.scitotenv.2022.155332

Science of the Total Environment 834 (2022) 155332

Contents lists available at ScienceDirect

Science of the Total Environment

journal homepage: www.elsevier.com/locate/scitotenv

Retention of immobile Se(0) in flow-through aquifer column systems during bioreduction and oxic-remobilization

Mallory S. Ho [a], Gianni F. Vettese [a], Katherine Morris [b,*], Jonathan R. Lloyd [b], Christopher Boothman [b], William R. Bower [a], Samuel Shaw [b], Gareth T.W. Law [a,**]

[a] Radiochemistry Unit, Department of Chemistry, University of Helsinki, 00014, Finland
[b] Department of Earth and Environmental Sciences, University of Manchester, M13 9PL, UK

HIGHLIGHTS

- Long-term (170 day) Se transport and retention examined in bioreducing columns
- Se(VI)(aq) forms sediment associated Se (0) during bioreduction, colloids not found
- Perturbation experiments (oxic groundwater/seawater) then conducted for 170 days
- Limited (<20%) Se(0) remobilization observed in perturbation experiments
- Past sulfidic conditions seem to enhance overall Se(0) retention.

GRAPHICAL ABSTRACT

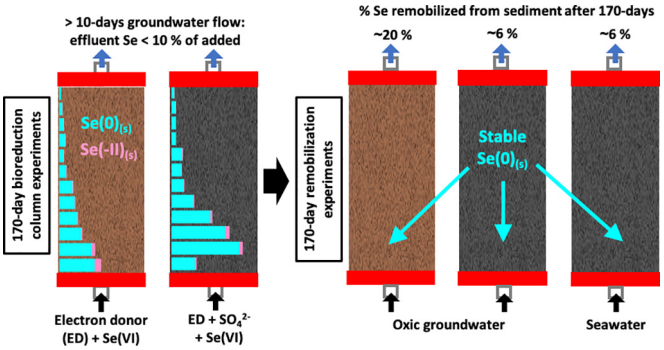

ARTICLE INFO

Editor: Mae Sexauer Gustin

Keywords:
Contaminated land
Geological disposal
Biostimulation
XAS
Sequential extraction

ABSTRACT

Selenium (Se) is a toxic contaminant with multiple anthropogenic sources, including ^{79}Se from nuclear fission. Se mobility in the geosphere is generally governed by its oxidation state, therefore understanding Se speciation under variable redox conditions is important for the safe management of Se contaminated sites. Here, we investigate Se behavior in sediment groundwater column systems. Experiments were conducted with environmentally relevant Se concentrations, using a range of groundwater compositions, and the impact of electron-donor (i.e., biostimulation) and groundwater sulfate addition was examined over a period of 170 days. X-Ray Absorption Spectroscopy and standard geochemical techniques were used to track changes in sediment associated Se concentration and speciation. Electron-donor amended systems with and without added sulfate retained up to 90% of added $Se(VI)_{(aq)}$, with sediment associated Se speciation dominated by trigonal Se(0) and possibly trace Se(-II); no Se colloid formation was observed. The remobilization potential of the sediment associated Se species was then tested in reoxidation and seawater intrusion perturbation experiments. In all treatments, sediment associated Se (i.e., trigonal Se(0)) was largely resistant to remobilization over the timescale of the experiments (170 days). However, in the perturbation experiments, less Se was remobilized from sulfidic sediments, suggesting that previous sulfate-reducing conditions may buffer Se against remobilization and migration.

1. Introduction

Selenium (Se) is an essential micronutrient for human and animal health (Kieliszek and Błazejak, 2013); however, it also has one of the narrowest concentration ranges between dietary deficiency (<40 μg/day) and toxicity (>400 μg/day) (Kieliszek and Błazejak, 2013; WHO

* Correspondence to: K. Morris, Research Centre for Radwaste Disposal, Department of Earth and Environmental Sciences, The University of Manchester, Manchester M13 9PL, UK.
** Correspondence to: G.T.W. Law, Radiochemistry Unit, Department of Chemistry, The University of Helsinki, A.I Virtasen Aukio 1, Helsinki 00560, Finland.
E-mail addresses: katherine.morris@manchester.ac.uk (K. Morris), gareth.law@helsinki.fi (G.T.W. Law).

http://dx.doi.org/10.1016/j.scitotenv.2022.155332
Received 25 February 2022; Received in revised form 12 April 2022; Accepted 12 April 2022
Available online 20 April 2022

Technical Report Series, 1973). Se concentrations in soils and sediments typically range between 0.01 and 2.00 mg/kg (Fairweather-Tait et al., 2011). Several factors including source geology, sediment biogeochemistry, and anthropogenic Se sources can result in highly elevated Se concentrations in the geosphere (1000–10,000 mg/kg) (Fishbein, 1983), presenting a hazard to ecosystems and human health (Kieliszek and Błazejak, 2013; WHO Technical Report Series, 1973). As a consequence, Se is considered a contaminant of major global concern (Kieliszek and Błazejak, 2013; WHO Technical Report Series, 1973; Sandy and DiSante, 2010). Se has multiple anthropogenic sources, for example, fossil fuel combustion, mining, crude oil refining, civil works, and agricultural irrigation of seleniferous soils (for further information, see Tamoto et al., 2015 and the review by He et al., 2018). A radioisotope of Se (^{79}Se, half-life ~3.27 $\times 10^5$ years, β^- decay energy = 0.1506 MeV) is also present at significant levels in higher activity radioactive wastes produced from nuclear fission reactions. The international consensus is that these wastes will be managed via disposal in a deep geological disposal facility (GDF) (Morris et al., 2010; World Nuclear Association, n.d.). However, given the long half-life of ^{79}Se, it may eventually be transported out from the engineered barrier toward the biosphere. Consequently, Se is a critical element both in geodisposal biosphere safety assessments and in contaminated land studies. As such, it is important that Se biogeochemistry is well understood.

Se transport, bioavailability, and toxicity in the environment largely depend on its oxidation state. Under environmentally relevant conditions, Se has access to four oxidation states: Se(VI), Se(IV), Se(0), and Se(-II) (Tan et al., 2016). Under oxic conditions and mildly acidic to alkaline pH, Se speciation is dominated by the Se(VI) and Se(IV) oxyanions, selenate (SeO_4^{2-}) and selenite (SeO_3^{2-}), respectively. These are the most mobile, bioavailable, and toxic forms of Se (He et al., 2018; Masscheleyn and Patrick, 1993). Under reducing conditions, poorly soluble elemental selenium (Se(0)) and selenide (Se(-II)) species become prevalent (Tan et al., 2016; Lenz et al., 2008).

Se migration through the geosphere is hindered by sorption and incorporation reactions with clay minerals and other mineral phases, particularly to aluminum, manganese, and iron oxides (Hayes et al., 1987; Peak and Sparks, 2002; Peak, 2006; Saeki et al., 1995; Séby et al., 1998; Tabelin et al., 2014). Alternatively, Se(VI/IV) can also be immobilized by reduction to lower, poorly soluble oxidation states such as Se(0) or Se(-II) (Ikonen et al., 2016). Fe(II)-bearing minerals are potential candidates for abiotic reduction of Se(VI/IV) (Séby et al., 1998; Myneni et al., 1997; Scheinost and Charlet, 2008). Indeed, the abiotic reduction of Se(IV) by mackinawite (FeS), magnetite (Fe_3O_4), and siderite ($FeCO_3$) has been shown to create a range of poorly soluble Se products (red monoclinic Se (0), grey trigonal Se(0), Fe_7Se_8, and FeSe, depending on Fe(II)-bearing phases and pH) (Scheinost and Charlet, 2008). However, some of these phases form nanoscale clusters, and there has been suggestion that this could result in colloid-facilitated Se transport (Scheinost and Charlet, 2008).

Whilst abiotic reduction of Se(VI/IV) is clearly possible, formation of Se (0) or Se(-II) in the biosphere is thought to be mainly mediated by microorganisms (Nancharaiah and Lens, 2015; Pearce et al., 2009; Lusa et al., 2019). Microbes can use Se(VI/IV) oxyanions as terminal electron acceptors in energy metabolism (dissimilatory reduction) or they can reduce and incorporate Se into a range of organic compounds (assimilatory reduction) (Fernández-Martínez and Charlet, 2009). They also reduce Se(VI/IV) as a detoxification mechanism (Garbisu et al., 1995; Lortie et al., 1992), to maintain redox potential (Kessi et al., 1999), to incorporate Se into the cell as an essential cofactor (Zoidis et al., 2018), and/or as part of a respiratory electron transfer chain (Klonowska et al., 2005; Switzer Blum et al., 1998). The (bio)chemical similarities between Se and sulfur (S) also mean that the presence of both sulfate and sulfate-reducing bacteria (SRB) can significantly impact Se biogeochemistry (Hockin and Gadd, 2003; Zehr and Oremland, 1987; Geoffroy and Demopoulos, 2010; Oremland et al., 1989). Interestingly, in pure culture experiments, a number of microbes have been shown to reduce Se(VI/IV) to form Se(0) nanoparticles (Kessi et al., 1999; Losi and Frankenberger, 1997; Oremland et al., 2004). The physicochemical properties of these nanoparticles (size, shape, morphology, crystal structure, and surface charge) strongly affect Se(0) colloid stability and settling behavior, which in turn can influence the mobility and bioavailability of Se (Oremland et al., 2004; Jain et al., 2017; Ruiz Fresneda et al., 2018). For example, Ruiz Fresneda et al. (2018) (Ruiz Fresneda et al., 2018) demonstrated that the reduction of Se(IV) resulted in the formation of 30–200 nm sized amorphous monoclinic Se(0) nanoparticles, which then transformed into the less soluble, 30–400 nm sized trigonal Se(0) nanoparticles. Many investigations have reported that monoclinic Se(0) nanoparticles typically form “8-rings”, where Se can coordinate with S atoms to form $Se_{8-n}S_n$ structured nanoparticles (suggesting that S is involved in their formation) (Fernández-Martínez and Charlet, 2009; Geoffroy and Demopoulos, 2010; Jain et al., 2017; Ruiz Fresneda et al., 2018; Vogel et al., 2018). These $Se_{8-n}S_n$ nanoparticles are colloidally stable because of their negative surface charge, potentially making them mobile in the environment (Vogel et al., 2018).

At present, the redox stability and pathways of reduced Se phases (including Se(0) nanoparticles) in the environment are poorly defined, although some microorganisms are known to be capable of oxidizing Se (0) and Se(-II) species to Se(VI) or Se(IV) (Zhang et al., 2004; Buchs et al., 2013). Interestingly, these oxidation reactions appear to be kinetically slow (~10^3 times slower than bioreduction), but importantly, oxidation could lead to possible remobilization of sediment associated Se(0) and/or alteration of Se nanoparticles (Zhang et al., 2004; Dowdle and Oremland, 1998).

Whilst Se species clearly displays complex behavior in environmental systems, most current understanding of Se biogeochemistry stems from pure culture, microcosm, or mineral sorption studies. Here, elevated $Se_{(aq)}$ concentrations are often used, and many of the complexities of the (bio) geosphere are lacking (e.g., groundwater flow, concentration and redox gradients/fluctuations, the presence of complex microbial communities, and extended time scales). Furthermore, the longer-term behavior of Se during redox-cycling and/or seawater intrusion is poorly constrained (Masscheleyn and Patrick, 1993; Wiramanaden et al., 2010; Weres et al., 1989). Here, the intrusion of oxic waters (e.g., shallow/deep groundwater or seawater) could reoxidize the geosphere, alter pH, and/or in the case of seawater, significantly alter ionic strength (Eagling et al., 2013).

Reflecting the above, the objective of our work was to better document the behavior and speciation of Se under realistic environmental conditions (with groundwater flow) over several months, using relevant $Se_{(aq)}$ concentrations, and complex experimental matrices (real sediment with groundwaters of varying composition). This was achieved through use of sediment and flowing groundwater column systems (Bower et al., 2019; Thorpe et al., 2016). Specifically, we sought to examine Se-retention and remobilization mechanisms, and the potential for nanoparticle production and transport under different groundwater conditions (bioreducing conditions with and without sulfate reduction, oxidizing conditions, and seawater intrusion) in complex aquifer materials representative of nuclear legacy sites.

2. Materials and methods

2.1. Sediment and synthetic groundwater/seawater

Sediment was collected from a site next to the Calder River, Cumbria, UK (Lat 54°26′30 N, Long 03°28′09 W) which has been well characterized, and used extensively in radionuclide biogeochemistry/contaminant studies relevant to the UK nuclear legacy (Bower et al., 2019; Law et al., 2010; Thorpe et al., 2017; Masters-Waage et al., 2017). On collection, large stones were handpicked from the sediment, and the remaining material was stored in sterile, HDPE bags. Sediment was stored at 10 °C in the dark until use. Autoclaved synthetic groundwater/seawater was used in experiments at pH 7 (SI Table S1 and S2) (Masters-Waage et al., 2017; Wilkins et al., 2007). Sediment characteristics (including information on mineralogy and elemental composition) are fully described in SI Section 2. Briefly the sediment mineralogy was dominated by quartz, sheet silicates, feldspars,

and Fe-oxides, and the sediment contained 6.5 wt% Fe, and no measurable Se. All chemicals were of analytical grade.

2.2. Column design and experimental approach

A sediment column system with flowing groundwater (based on that of Bower et al., (2019)) (Bower et al., 2019) was used to explore Se behavior under dynamic environmental conditions. A schematic of the column setup can be found in SI Fig. S1. Briefly, a 10 cm polypropylene column with 1 cm inner diameter was terminated on each end with layers of glass wool (1 cm vertical) and quartz sand (1 cm vertical), whilst the remaining space in the column (6 cm vertical) was packed tightly with sediment (~8 g). The columns were then sealed with Bola GL14 screw caps. A peristaltic pump was used to pump groundwater into the base of the columns at a flowrate of 0.5 ± 0.1 mL/h (Thorpe et al., 2017; Sellafield Ltd, 2016). Effluent was periodically collected from the top of the columns by attaching a syringe to the outlet of a 3-way valve.

Three Se amended synthetic groundwater compositions were used in the study: (i) an oxic system with no electron-donor amendments, (ii) an electron-donor amended system, and (iii) an electron-donor + sulfate amended system (SI Table S1). Se(VI) (as Na_2SeO_4) was continually added to the influent groundwaters of these systems at a concentration of 5 μM (Tan et al., 2016). The oxic system was used to examine Se(VI) behavior under fully oxic groundwater conditions; here, an air-bubbler was used to maintain O_2 in the influent. The electron-donor amended, and electron-donor + sulfate amended systems were used to examine Se behavior under different bioreducing conditions (such that one system would support sulfate reduction, the other not), and later, under perturbation scenarios where the influent was changed to simulate the intrusion of oxic ground or seawater.

To promote bioreduction, 2 mM of acetate and 2 mM of lactate were added to both bioreducing groundwater systems. The electron-donor amended system had no added sulfate. In contrast, to examine the impact of sulfate on Se behavior during bioreduction, 0.4 mM of sulfate was added to the electron-donor + sulfate amended groundwater (SI Table S1). All groundwater systems also contained 0.3 mM NO_3^-. Both bioreducing groundwater systems were continually sparged with Ar before being pumped through the columns. All the column systems were then reacted under constant flowing conditions for 170 days, in the dark, at 21 ± 2 °C.

Additional electron-donor amended and electron-donor + sulfate amended column systems (as described above) were reacted for 170 days and these columns were used in later perturbation experiments to examine whether any Se that may have become associated with the sediment could be remobilized. Accordingly, at the end of the bioreduction groundwater treatments, the influent solution to these columns was changed to either oxic groundwater (as described before) or synthetic, oxic seawater (SI Table S2). An air-bubbler was used to maintain aerobic conditions in the influent solutions. Further, the influents had no added Se and were pumped through the columns at the same flow rate of 0.5 ± 0.1 mL/h.

2.3. Sampling, column sacrifice, and geochemical characterization

Duplicate columns were run for all groundwater systems (excluding perturbation experiments with oxic groundwater/seawater) and effluent samples were collected at regular intervals under anoxic conditions (Ar flushing). Subsequent sample handling was also under anoxic conditions (Ar filled glove bag). After collection, the samples were centrifuged at $1.4 \times 10^4 g$ for 5 min to separate the solids and supernatant. Then, to further understand microbially mediated terminal electron accepting processes, changes in sediment geochemistry, and Se behavior/migration, the supernatant was characterized. Effluent pH and Eh were measured using calibrated electrodes (Mettler-Toledo). Effluent NO_2^-, HS^-, and Fe were measured spectrophotometrically (Stookey, 1970; Grasshoff et al., 1999; Viollier et al., 2000; Townsend et al., 2020). Additionally, NO_3^-, SO_4^{2-}, and Br^- (added as an inert tracer) were measured by ion chromatography (Metrohm Eco IC). Mn and Se concentrations were measured by inductively coupled plasma mass spectrometry (ICP-MS) (Agilent 7800) from acidified (0.5% HNO_3) samples. The possible presence of Se nanoparticles (or other colloids) in the effluent was also assessed through use of dynamic light scattering (DLS) and zetapotential analysis (Malvern Zetasizer nanoZS).

At experiment endpoints (170 days of bioreducing treatment with or without sulfate addition, or after an additional 170 days of oxic groundwater / seawater treatment), columns were transferred into an Ar-filled glove bag. The columns were then uncapped, sliced along their length, and sectioned at 0.5 cm intervals. The resulting sectioned samples were stored under an Ar atmosphere, at −80 °C, prior to solid phase analysis (X-ray absorption spectroscopy analysis and 16S rRNA gene sequencing). The sediment structure and the possible presence of immobilized Se nanoparticles/discrete Se phases in the sediment matrix were also assessed using field emission scanning electron microscopy with energy dispersive X-ray spectroscopy (FESEM-EDX) (Hitachi S-4800 and Oxford INCA 350 EDS). The sectioned materials were also analyzed by: (i) digestion in boiling *aqua regia* (4 h) for elemental analysis by ICP-MS to estimate total Fe and Se retention (for select samples to inform later XAS analysis), and (ii) leaching in 0.5 N HCl for 1 h to estimate the proportion of bioavailable Fe (II) (as a percentage of total extractable Fe) in the treated sediments (Lovley and Phillips, 1987). Additionally, sequential extractions were completed on sectioned sediment samples to explore differences in Se geochemical partitioning as operationally defined by the extraction lixiviants (Wright et al., 2003). Specifically, the sequential extraction included a 2 h extraction with 0.25 M KCl (targeting soluble/exchangeable Se(VI)), a 2 h extraction with 0.1 M K_2HPO_4 (targeting adsorbed Se(IV)), a 4 h extraction completed in an ultrasonic bath with 0.25 M Na_2SO_3 (targeting elemental Se(0)), and a 30 min extraction at 90 °C with 5% NaOCl (targeting a mixture of organically associated Se(-II) and metal selenide forms (e.g., FeSe)) (Wright et al., 2003). A final extraction with boiling *aqua regia* for 4 h was completed to target any remaining sediment associated Se. All extraction chemicals were thoroughly sparged with Ar before use.

2.4. X-ray absorption spectroscopy (XAS)

Se speciation and local coordination in the sediment was investigated using X-ray absorption near edge structure (XANES) and extended X-ray absorption fine structure (EXAFS) analysis. XAS data were collected from select samples with a 64 element Ge detector with an in-line Pb foil for energy calibration on beamline I20 at Diamond Light Source, UK, from the Se K-edge in fluorescence mode at 77 K. In the Demeter software package, background subtraction, normalization of data, and linear combination fitting (LCF) of XANES between Se standards (Se(VI), Se(IV), trigonal Se(0), monoclinic Se(0), and Se(-II)) was completed in Athena (Ravel and Newville, 2005). EXAFS spectra were fit shell by shell in Artemis, using relevant information from the literature (Ravel and Newville, 2005; Ryser et al., 2005; Breynaert et al., 2008). Here, F-testing was used to determine the statistical viability of adding backscattering shells (Downward et al., 2009). The fitting procedure was constrained to fixed values for the passive electron reduction factor (S_0^2) and Debye − Waller factor (σ^2) to determine the trend in Se coordination number (CN) for the various oxidation states.

2.5. DNA extraction and microbial community characterization

Changes in the microbial community structure during experiments were examined by extracting DNA from select sediment samples from each system and amplifying and sequencing 16S rRNA genes from the extant microbial communities (Macaulay et al., 2020; Ruiz-Lopez et al., 2020). Further details are provided in SI Section 4.

3. Results and discussion

3.1. Column effluent geochemistry and microbial ecology

Three different Se amended groundwater systems ((i) oxic (no electron donor), (ii) electron-donor amended, and (iii) electron-donor + sulfate amended) were pumped through parallel, duplicate sediment columns for

170 days. The effluent pH from all of the column systems buffered to 7–8, likely due to bicarbonate alkalinity in the influent groundwaters or alkalinity generation in the microbially active treatments, which is similar to work by Bower et al. (2019) who used sediment from the same site. In the oxic control system, the effluent Eh (SI Fig. S3) remained at approximately +250–350 mV throughout the experiment in both columns. Small amounts of NO_2^- (SI Fig. S5) were present in the effluent, but Mn (SI Fig. S6), Fe (SI Fig. S7), and HS^- (SI Fig. S9) were either very low or not detected; as such, the system treated with oxic groundwater maintained oxic/denitrifying conditions, but did not support microbially-mediated metal or sulfate reduction (NO_3^- was not measured in the oxic system effluents). In the effluent, ~90% of added Se remained in the effluent (Fig. 1, SI Table S3). This is consistent with Se(VI) behavior under oxic conditions, where soluble Se(VI) oxyanions show limited sorption to geomedia at pH >7.5 (Tan et al., 2016; Masscheleyn and Patrick, 1993; Séby et al., 1998; Jayaweera and Biggar, 1996). Under denitrifying conditions, previous studies (Tan et al., 2016; Oremland et al., 1999) have reported that denitrifying bacteria can enhance microbial SeO_4^{2-} removal; this did not seem significant in the oxic system given continual Se output in the effluents (Fig. 1).

To study the behavior of Se under bioreducing subsurface conditions, acetate and lactate (2 mM) were continually supplied in the influent groundwater of the electron-donor amended and the electron-donor + sulfate amended systems for 170 days. The trends in the effluent groundwater chemistry (SI Section 5) indicated that a cascade of microbially-mediated terminal electron accepting processes occurred. In both of these bioreducing systems, NO_3^- was added at a constant concentration of 0.3 mM. After an initial 24 h period of NO_3^- elution, there was a gradual decrease of NO_3^- in the effluents to low concentrations (<30 μM) in the electron-donor amended system, and with concentrations below the detection limit for the electron-donor + sulfate amended system (SI Fig. S4). Also, low but detectable NO_2^- (SI Fig. S5) was present in the effluents of both systems until the end of the experiment. This suggests that dissimilatory NO_3^- reduction was measurable after 1 day in these systems. It is likely that a stable denitrifying community had developed in the columns, consistent with results from similar experiments (Bower et al., 2019; Law et al., 2010).

After denitrification in both systems, microbially-mediated metal-reducing conditions were then observed, with Mn (SI Fig. S6) appearing in the effluent from 1 to ~50 days and Fe (SI Fig. S7) appearing after ~10 days. These geochemical signals were further supported by the increase in dissimilatory metal-reducing bacteria in both of the bioreducing systems, compared to the fresh sediment (SI Fig. S2). Again, this reflects the results from past studies with similar materials (Bower et al., 2019; Law et al., 2010).

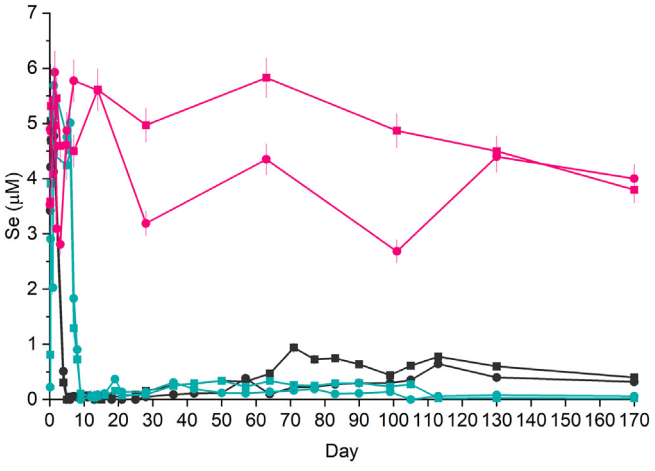

Fig. 1. Concentration of Se in effluents for 3 different groundwater systems: (pink) oxic (no added electron-donor), (green) electron-donor amended, and (black) electron-donor + sulfate. Each system was conducted in duplicate and thus shows variability per system; individual columns (per system) are represented by squares and circles. Error bars = 1 σ combined analytical error. Where error bars are not visible, they are within the symbol size.

In the electron-donor amended system (with no added sulfate), neither SO_4^{2-} (SI Fig. S8) nor HS^- (SI Fig. S9) were detected in the effluent which is consistent with the geochemistry of the influent groundwater. However, in the electron-donor + sulfate system there was clear evidence for robust sulfate-reduction. First, from 0 to 15 days there was a decrease in effluent SO_4^{2-} concentrations from 400 μM on day 0, to below the detection limit (0.7 μM) on day 15 (SI Fig. S8). Second, HS^- was detected in the effluent after ~10 days until the end of the reaction period (170 days), indicating that SO_4^{2-} was being reduced to HS^- and was likely retained in the sediment for part of the reaction period (e.g., by precipitation of metal sulfides) (Berner, 1967). Finally, there was also a detectable sulfide odor and a noticeable blackening of sediment sections.

In both bioreducing systems, >90% of the Se, added as Se(VI), had been removed (SI Table S3) from the groundwater by the end of the experiment. Further, Se was eluted for a total of ~10 days from both column treatments, and the Se concentration in the effluents started to decrease after ~3 days (Fig. 1). In comparison, breakthrough of the conservative Br^- tracer occurred within the first 10 h (SI Fig. S10), indicating that Se transport in the columns was significantly retarded under bioreducing conditions. Indeed, after ~10 days, Se in the effluents remained <1 μM of both bioreducing systems to the experimental endpoint (170 days). This suggests that the presence of elevated sulfate in the electron-donor + sulfate amended system did not affect overall Se retention during bioreduction when compared to the electron-donor amended system, consistent with previous studies (Zehr and Oremland, 1987). However, we note that toward the end of the experiments (105–170 days), a slightly elevated level of Se was eluted from the electron-donor + sulfate amended system (0.30–0.80 μM) compared to the electron-donor system (0.02–0.30 μM) (Fig. 1). This could be due to the presence of more mobile HSe^- species in this more reducing system (e.g., Herbel et al., 2003) or elevated ionic strength effects from the added sulfate (e.g., Zehr and Oremland, 1987; Söderlund et al., 2016; Dowdle and Oremland, 1998; Hockin and Gadd, 2003, 2006; Tan et al. 2018; Séby et al. 1998) (Séby et al., 1998; Hockin and Gadd, 2003; Zehr and Oremland, 1987; Dowdle and Oremland, 1998; Söderlund et al., 2016; Hockin and Gadd, 2006; Tan et al., 2018). Further work is needed to clarify this.

Based on these effluent data alone, numerous pathways may lead to Se retention. It is likely that Se(VI) was initially eluted from both systems due to its weak sorption characteristics under the initial ~10 days where oxic/denitrifying conditions dominated in the columns. Then, the gradual decrease of Se in effluent over ~10 days in both systems is likely a result of active reduction of Se(VI) to its lower, poorly soluble oxidation states. This was further explored by analysis of the Se concentration and speciation in sediments from these columns.

3.2. Solid phase geochemistry

3.2.1. Acid digests and sequential extractions

After 170 days of constant groundwater flow, sediment columns from the electron-donor amended and electron-donor + sulfate amended systems were sectioned at 0.5 cm intervals under O_2-free conditions. The concentration of sediment associated Se in the sediment sections were measured in sequential extraction lixiviants to study differences in Se retention, migration, and speciation under the different groundwater systems and relative to the sediment geochemistry. To support this, the concentration of 0.5 N HCl extractable Fe(II) (as a percentage of total 0.5 N HCl extractable Fe) was also measured in sediments.

In the oxic system with no electron donor amendments, trace amounts (~2%) of the 0.5 N HCl extractable Fe was present as Fe(II). By contrast, in both of the bioreducing systems (with and without sulfate), sediment >0.5 cm from the groundwater inlet had >80% of the 0.5 N HCl extractable Fe present as Fe(II) (Fig. 2), confirming significant reduction of bioavailable Fe(III) to Fe(II) and extensive retention of Fe(II) in the sediment. This is consistent with the aqueous geochemistry (SI Section 5) and microbial ecology

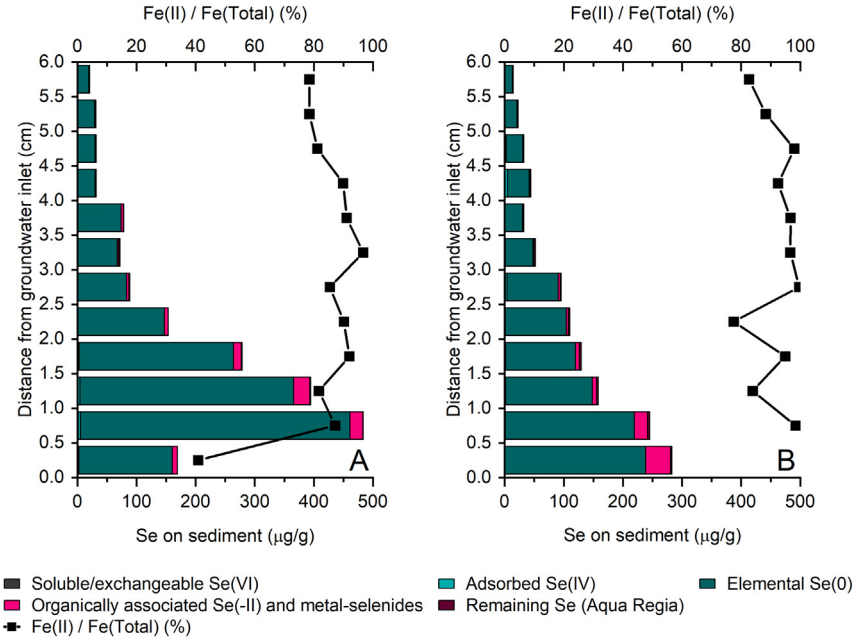

Fig. 2. Concentration of Se on sediment extracted per lixiviant (see key) and 0.5 N HCl extractable Fe(II) expressed as a % of total 0.5 N HCl extractable Fe from selected sediment samples (0.5 cm depth increments) from: (A) the electron-donor amended system, and (B) the electron-donor amended + sulfate system. Note there was not enough sediment to measure the Fe(II) in the 0–0.5 cm sample in the electron-donor + sulfate system.

data (SI Section 4). Interestingly, in the section closest to the groundwater inlet (0–0.5 cm) in the electron-donor amended column, only ~40% 0.5 N HCl extractable Fe(II) was measured, suggesting that this section was not as reducing as the rest of the column. This may be due to the constant input of groundwater NO_3^- (e.g., establishment of a stable denitrifying zone or redox reactions between NO_2^- and Fe(II)). Unfortunately, there was not enough sediment for an equivalent measurement from the electron-donor + sulfate amended system.

In both bioreducing systems, sediment associated Se was detected throughout each column, with the total Se concentrations (sum of Se in all lixiviants) in individual sections varying between ~10 and ~500 μg of Se per g of sediment (Fig. 2). The general trend of Se retention in both column systems, with and without sulfate, showed that in both systems, ~70% (SI Table S4) of Se was retained within 2 cm of the groundwater inlet, with only limited Se retention (up to 9%) to the upper part of the column (>4 cm beyond the groundwater inlet). Interestingly, less Se was associated with sediments within 0.5 cm of the inlet in the electron-donor amended system, which was not as reducing as the rest of the column (Fig. 2), suggesting that stronger reducing conditions increases the rate of Se retention. Regardless, in both bioreducing systems, sequential extractions (Fig. 2, SI Table S4) indicated that the majority (up to 99% in an individual section) of sediment associated Se was present in the Na_2SO_3 fraction, presumptively as elemental Se(0), and that up to 15% of Se in an individual section was in the NaOCl fraction, suggesting there may be formation of a mixture of organically associated Se(-II) and metal-selenides.

Interestingly, Ruiz-Fresneda et al. (2019) (Ruiz-Fresneda et al., 2019) proposed that when Se(IV) was exposed to pure cultures of *Stenotrophomonas bentonitica*, monoclinic Se(0) nanoparticles attached and accumulated on organic matter within 48–72 h, forming trigonal Se(0) particles after 144 h. Reduced Se has also been shown to form nanoclusters that may be subject to colloidal transport (Scheinost and Charlet, 2008). In our work, aqueous phase analysis using dynamic light-scattering and zetapotential analysis did not show evidence of Se nanoparticles in solution. Further, extensive SEM surveys of the solids from experiment endpoints (where Se concentrations were up to ~500 mg/kg in the bulk) did not show presence of any discrete Se phases (e.g., Se(0) nanoparticles). This is perhaps unsurprising given the aqueous Se concentration difference between the column experiments presented here (5 μM Se) and that used in the past studies (0.1–1.0 mM Se (Ruiz-Fresneda et al., 2019); 0.99–9.09 mM Se (Scheinost and Charlet, 2008)).

In summary, sequential extraction results indicated that an active zone of Se(VI) removal developed close to the groundwater inlet in each bioreducing system, and that sulfate amendment did not significantly impact Se speciation in the sediments as both systems showed similar Se distributions. Overall, this suggests that Se immobilization in both systems was independent of sulfate concentration in the influent, and was controlled by reaction to reduced, poorly soluble Se during microbially-mediated Mn(IV/III) and Fe(III)-reduction rather than during sulfate-reduction. Indeed, the abiotic reduction of Se(VI/IV) oxyanions by Fe(II)-bearing minerals most commonly produces Se(0), and precipitation of metal-selenides has only been shown in mineral sorption / pure culture experiments (Scheinost and Charlet, 2008; Breynaert et al., 2008; Pearce et al., 2008), which is consistent with the relatively small amounts of the organically associated Se(-II) and metal-selenides observed in the sequential extraction data.

3.2.2. Speciation of Se associated with sediment

Se K-edge XAS was used to determine the Se oxidation state and local coordination environment in select samples from the electron-donor amended and electron-donor + sulfate amended systems. The absorption edge energy and the shape of Se K-edge XANES are related to Se oxidation state and molecular structure. Although this is a useful tool for distinguishing Se in different oxidation states, elemental Se(0) has two major allotropes (amorphous monoclinic and crystalline trigonal) which are not easily discerned using XANES (Lenz et al., 2008).

XANES data (SI Fig. S11) were obtained for three sediment sections for both of the bioreducing systems ((i) 0–0.5 cm, (ii) 0.5 cm–1.0 cm, and (iii) 4.0 cm–4.5 cm). All XANES spectra (SI Fig. S11) aligned with the two Se (0) reference standards and none of the sediment spectra were consistent with Se(VI) or Se(IV) standards. Although up to 15% of Se(-II) was observed in the sequential extraction lixiviants (Fig. 2) for an individual section, the XANES spectra from the samples did not show evidence for the significant presence of Se(-II) (SI Fig. S11).

EXAFS data were collected to directly investigate the local coordination of Se in the sediments and to explore whether different Se(0) allotropes were present. Results from the fits to the EXAFS from the monoclinic and

trigonal Se(0) standards (SI Table S5 and S6) indicate a 1st shell of Se-Se backscatterers at 2.3 Å for both Se(0) standards (CN of 2), and a 2nd shell of Se-Se backscatterers at 3.4 Å (CN of 4) and 3.7 Å (CN of 1) for trigonal and monoclinic Se(0), respectively. The 3rd Se-Se shell for trigonal Se (0) at 3.7 Å (CN of 2) was also fitted (Breynaert et al., 2008). Fig. 3 compiles the EXAFS spectra and fits for the monoclinic Se(0) standard, the trigonal Se (0) standard, and selected sediment samples.

In all the bioreduced sediment samples, the 1st shell in the Fourier transform of the EXAFS for all the samples was fit as a Se-Se shell at 2.3 Å (CN of 2), consistent with both monoclinic and trigonal Se(0) (SI Tables S5 and S6; Fig. 3). Subsequent fitting of the 2nd and 3rd shells (at 3.4 Å and 3.7 Å with CN of 4 and 2, respectively) confirmed Se was present as Se(0) in trigonal, rather than monoclinic geometry, in all samples (SI Table S5). The addition of these shells statistically improved the fits by more than 2 standard deviations (F-test >95%) (Marshall et al., 2014) and provided better fits than those informed by monoclinic Se(0) geometry (SI Table S6). Attempts to add ~15% of FeSe(-II) with a Se-Fe backscattering shell at 2.38 Å, and a Se-Se backscattering shell at 3.71 Å, and/or selenomethionine with a Se-C backscattering shell at 1.95 Å, did not improve or yield satisfactory fits. This suggests that the bioreduced sediment samples predominately contained precipitated (i.e., discrete) or sorbed trigonal Se(0), consistent with the sequential extractions and XANES, further indicating that sulfate did not significantly affect the speciation of Se after reduction (Scheinost and Charlet, 2008; Breynaert et al., 2008; Pearce et al., 2008).

3.3. Perturbation experiments

Considering the long half-life of ^{79}Se, it is expected to be a contaminant radionuclide for >10^5 years (He et al., 2018). During this time, environmental perturbations to reduced sediments may arise following the intrusion of, for example, oxic groundwaters (promoting oxidation) and/or seawater (which may impact salinity) (Duro et al., 2014; Singleton et al., 2005; Burke et al., 2006). Further, in Se contaminated aquifers, redox conditions and groundwater salinity can be ephemeral. To explore the stability of bioreduced Se, perturbation experiments were conducted for a further 170 days on Se-labelled bioreduced sediment columns from the electron-donor amended and electron-donor + sulfate amended systems (specifically, one electron-donor amended column was reoxidised with oxic groundwater, and two electron-donor + sulfate amended columns were reoxidised: one with oxic groundwater and the other with oxic seawater). In all these experiments, no Se was added to the influent solution that was used to perturb the bioreduced sediment columns.

When the influent for all columns was changed to oxic groundwater or seawater, the effluent Eh (SI Fig. S3) increased to +250–400 mV over 5 days, indicating that the columns were oxidized during the experiment. Additionally, NO_2^- concentrations increased to ~13 μM in the effluents around day 10, but then dropped to 1–3 μM until the end of the experiments (SI Fig. S5). Mn and Fe concentrations in the oxic groundwater perturbation experiments remained <2 μM throughout; however, when the electron-donor + sulfate amended system was flushed with seawater, there was an initial spike of Mn (~30 μM) (SI Fig. S6) and Fe (~80 μM) (SI Fig. S7) during the first day. This was likely due to ion exchange reactions, given the increased ionic strength of the seawater influent. Mn and Fe concentrations then remained <2 μM in this system until the end of the experiment. Microbial community analysis further evidenced column reoxidation with a decrease in the relative abundance of SRB in the electron-donor + sulfate system after exposure of oxic groundwater (SI Fig. S2).

An initial spike of Se (Fig. 4) was observed in the column effluent from all systems when switching to the oxic groundwater or seawater (although this was less marked for the electron-donor + sulfate amended systems). This initial spike likely represented oxidative remobilization of a small amount of labile Se, or in the seawater system, ion exchange. After ~3 days, Se in the effluents from both the electron-donor + sulfate perturbation systems (i.e., oxic groundwater and seawater) stabilized at <0.5 μM. In comparison, the electron-donor amended system that was exposed to oxic groundwater eluted Se at a slightly higher concentration (~1 μM) from 3 days until the end of the experiment. As such, by the end of the

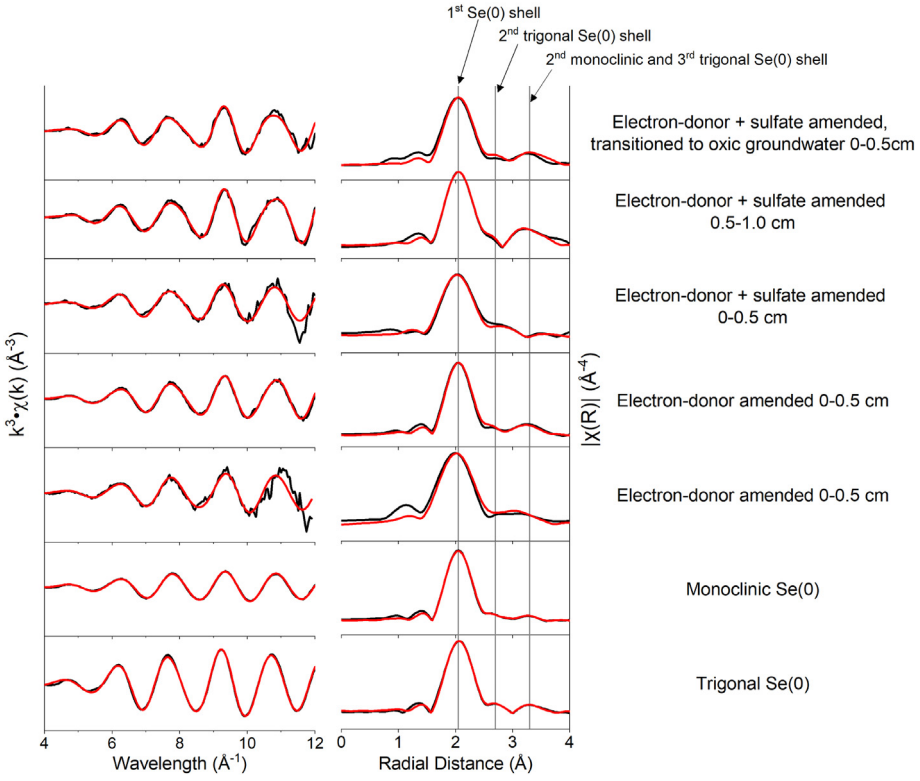

Fig. 3. Se K-edge EXAFS spectra for column sediment samples, Se(0) standards, and fits for k^3 weighted data (left) and their Fourier transforms (FT) (right). Fits are detailed in SI Table S5 and S6. Experimental data are shown in black, best fits (see SI) are in red.

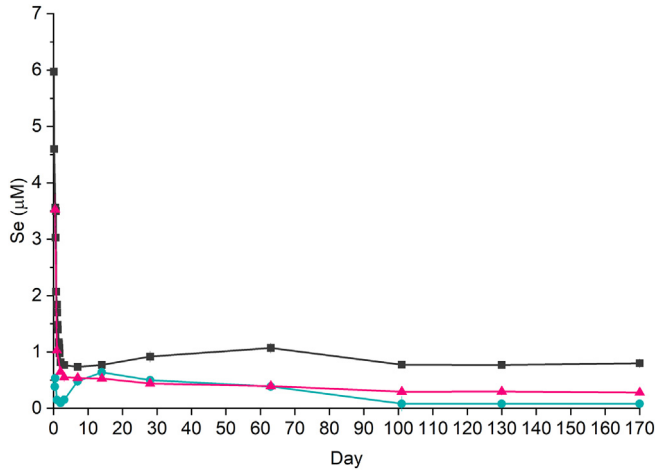

Fig. 4. Concentration of Se in effluents during 3 different perturbation experiments: (black squares) bioreduced sediments (170 days) from the electron-donor amended system, transitioned to oxic groundwater; (pink triangles) bioreduced sediments (170 days) from the electron-donor + sulfate system, transitioned to oxic groundwater; (green circles) bioreduced sediments (170 days) from the electron-donor + sulfate system, transitioned to oxic seawater. Error bars = 1 σ combined analytical error. When error bars are not visible, they are within the symbol size.

perturbation experiments, this system had remobilized the most Se (~20% of available Se) during the perturbation treatment. In comparison, the electron-donor + sulfate systems only remobilized ~6% of the sediment associated Se (SI Table S3).

XANES and EXAFS data for the 0–0.5 cm section of the electron-donor + sulfate amended column showed that trigonal Se(0) still dominated after 170 days, with no evidence for any other candidate of Se species in the EXAFS data (Fig. 3, SI Tables S5 and S6). This is consistent with other studies which showed that reoxidation of Se(0) and Se(-II) to Se (VI/IV) was up to 10^3 times slower than bioreduction (Hockin and Gadd, 2003; Oremland et al., 1989; Losi and Frankenberger, 1997; Jayaweera and Biggar, 1996).

Effluent data from these perturbation experiments suggests that Se retention in the electron-donor + sulfate system is significantly higher than in the electron-donor system that was not supplied with sulfate. XAS analysis further confirmed that Se speciation remained as trigonal Se(0) and unchanged from bioreduction systems after reoxidation. As sequential extraction and XAS analyses of bioreduced systems indicated that sulfate reduction did not significantly affect the speciation of Se, it seems the enhanced retention of Se in the sulfidic columns, under perturbation conditions, may be due to the formation of non-Se bearing sulfide phases (e.g., FeS), which, in turn, may act as a redox buffer against dissolved O_2, thus maintaining reducing conditions for longer compared to the bioreduced system without sulfate. Indeed, the redox buffer capacity of iron sulfides for a variety of subsurface contaminants (Séby et al., 1998; Scheinost and Charlet, 2008; Townsend et al., 2020; Marshall et al., 2014; Nakata et al., 2004; Fan et al., 2014) has been well documented.

4. Implications

Our experiments, conducted in dynamic sediment groundwater column systems, highlight the complexity of Se biogeochemistry as well as the importance of understanding biogeochemical processes in evolving, environmentally relevant systems. Effluent analysis showed that under oxic conditions, Se(VI) migration was significant with 90% of added Se(VI) transported through the column after 170 days. In contrast, anoxic conditions (stimulated by electron-donor and electron-donor + sulfate amendments) resulted in extensive Se immobilization (<10% of the added Se (VI) was transported through the columns during the bioreduction treatments). Here, Se(VI) removal and retention continued for up to 170 days under bioreducing conditions with or without added sulfate. Sequential extraction data indicated that Se(VI) was reductively scavenged, and XAS confirmed it predominantly formed trigonal Se(0) in the sediment. Interestingly, no Se colloid formation or transport was evident in any of the column systems but in future work, it would be interesting to further probe the chemistry of Se remaining in effluents from sediment column systems with varying redox chemistry.

Significant amounts of sediment associated Se were retained in subsequent perturbation experiments with oxic groundwater and seawater. The columns that had undergone sulfate-reducing conditions only remobilized <10% of the sediment associated Se. In contrast, ~20% of the sediment associated Se was remobilized when oxic groundwater was added into the electron-donor amended system (Fig. 4, SI Table S3), suggesting that Se retention is greater following sulfate-reducing conditions. This was attributed to redox buffering capacity from sulfide phases in the sediments. Interestingly, the rate of Se remobilization in oxic groundwater and seawater perturbations for the electron-donor + sulfate amended system was similar, suggesting that Se(0) remobilization was not significantly impacted by salinity (Fig. 4, SI Table S3). Our work demonstrates that bioreducing conditions can immobilize aqueous Se(VI) in dynamic column systems and suggests that sediments that develop sulfidic conditions may better limit Se transport if redox conditions change. Further, formation and/or transport of Se colloids in complex systems also seems less likely than in pure-culture systems. These observations have significant implications for Se environmental chemistry in contaminated environments.

CRediT authorship contribution statement

Study conceptualization: MSH, GTWL, KM, WRB.

Student supervision: GTWL, KM, WRB, GFV. Data collection, data processing, data interpretation: MSH, GTWL, KM, WRB, GFV, CB, JRL, SS. Manuscript writing and editing: MSH, GTWL, KM, GFV, JRL, CB, SS. Funding acquisition: GTWL and KM.

Declaration of competing interest

The authors declare no competing interests.

Acknowledgements

Mallory Ho acknowledges scholarship funding from the National Research Foundation, Singapore. Law, Morris, and Lloyd would like to acknowledge the EPSRC NNUF funded RADER Facility (EP/T011300/1), and NERC grant NE/M014088/1. Law and Vettese acknowledge funding from KYT2022 project VN/14858/2021. Diamond Light Source is thanked for beamtime allocation SP21441-3. We thank University of Helsinki staff members Juhani K. Virkanen and Hanna M. Reijola for technical assistance. SEM imaging and EDX measurements were completed on ALD Centre Finland research infrastructure.

Appendix A. Supplementary data

The Supporting Information contains additional information on sediment, influent water, microbial community characterization/composition, effluent groundwater chemistry, Eh data, and XAS data. Supplementary data to this article can be found online at https://doi.org/10.1016/j.scitotenv.2022.155332.

References

Berner, R.A., 1967. Thermodynamic stability of sedimentary iron sulfides. Am. J. Sci. 265 (9), 773–785.

Bower, W.R., Morris, K., Livens, F.R., Frederick, J., Mosselmans, W., Fallon, C.M., Fuller, A.J., Natrajan, L., Boothman, C., Lloyd, J.R., Utsunomiya, S., Grolimund, D., Ferreira Sanchez, D., Jilbert, T., Parker, J., Neill, T.S., Law, G.T.W., 2019. Metaschoepite dissolution in sediment column systems - implications for uranium speciation and transport. Environ. Sci. Technol. 53 (16), 9915–9925.

Breynaert, E., Bruggeman, C., Maes, A., 2008. XANES-EXAFS analysis of Se solid-phase reaction products formed upon contacting Se(IV) with FeS2 and FeS. Environ. Sci. Technol. 42 (10), 3595–3601.

Buchs, B., Evangelou, M.W.H., Winkel, L.H.E., Lenz, M., 2013. Colloidal properties of nanoparticular biogenic selenium govern environmental fate and bioremediation effectiveness. Environ. Sci. Technol. 47 (5), 2401–2407.

Burke, I.T., Boothman, C., Lloyd, J.R., Livens, F.R., Charnock, J.M., McBeth, J.M., Mortimer, R.J.G., Morris, K., 2006. Reoxidation behavior of technetium, iron, and sulfur in estuarine sediments. Environ. Sci. Technol. 40 (11), 3529–3535.

Dowdle, P.R., Oremland, R.S., 1998. Microbial oxidation of elemental selenium in soil slurries and bacterial cultures. Environ. Sci. Technol. 32 (23), 3749–3755.

Downward, L., Booth, C.H., Lukens, W.W., Bridges, F., 2009. A variation of the F-test for determining statistical relevance of particular parameters in EXAFS fits. AIP Conf. Proc. 882 (1), 129–131.

Duro, L., Domènech, C., Grivé, M., Roman-Ross, G., Bruno, J., Källström, K., 2014. Assessment of the evolution of the redox conditions in a low and intermediate level nuclear waste repository (SFR1, Sweden). Appl. Geochem. 49, 192–205.

Eagling, J., Worsfold, P.J., Blake, W.H., Keith-Roach, M.J., 2013. Influence of sediment redox conditions on uranium mobilisation during saline intrusion. Chem. Geol. 357, 158–163.

Fairweather-Tait, S.J., Bao, Y., Broadley, M.R., Collings, R., Ford, D., Hesketh, J.E., Hurst, R., 2011. Selenium in human health and disease. Antioxid. Redox Signal. 14 (7), 1337–1383.

Fan, D., Anitori, R.P., Tebo, B.M., Tratnyek, P.G., Lezama Pacheco, J.S., Kukkadapu, R.K., Kovarik, L., Engelhard, M.H., Bowden, M.E., 2014. Oxidative remobilization of technetium sequestered by sulfide-transformed nano zerovalent iron. Environ. Sci. Technol. 48 (13), 7409–7417.

Fernández-Martínez, A., Charlet, L., 2009. Selenium environmental cycling and bioavailability: a structural chemist point of view. Rev. Environ. Sci. Biotechnol. 8, 81–110.

Fishbein, L., 1983. Environmental selenium and its significance. Fundam. Appl. Toxicol. 3 (5), 411–419.

Garbisu, C., Gonzalez, S., Yang, W.H., Yee, B.C., Carlson, D.L., Yee, A., Smith, N.R., Otero, R., Buchanan, B.B., Leighton, T., 1995. Physiological mechanisms regulating the conversion of selenite to elemental selenium by Bacillus subtilis. Biofactors 5 (1), 29–37.

Geoffroy, N., Demopoulos, G.P., 2010. The elimination of Selenium(IV) from aqueous solution by precipitation with sodium sulfide. J. Hazard. Mater. 185, 148–154.

Grasshoff, K., Kremling, K., Ehrhardt, M., 1999. Methods of Seawater Analysis. 3rd ed. Wiley-VCH.

Hayes, K.F., Roe, A.L., Brown, G.E.J., Hodgson, K.O., Leckie, J.O., Parks, G.A., 1987. In situ X-ray absorption study of surface complexes: selenium oxyanions on Agr-FeOOH. Science 238 (4828), 783–786.

He, Y., Xiang, Y., Zhou, Y., Yang, Y., Zhang, J., Huang, H., Shang, C., Luo, L., Gao, J., Tang, L., 2018. Selenium contamination, consequences and remediation techniques in water and soils: a review. Environ. Res. 164, 288–301.

Herbel, M.J., Blum, J.S., Oremland, R.S., Borglin, S.E., 2003. Reduction of elemental selenium to selenide: experiments with anoxic sediments and bacteria that respire Se-oxyanions. Geomicrobiol. J. 20 (6), 587–602.

Hockin, S., Gadd, G.M., 2006. Removal of selenate from sulfate-containing media by sulfate-reducing bacterial biofilms. Environ. Microbiol. 8 (5), 816–826.

Hockin, S.L., Gadd, G.M., 2003. Linked redox precipitation of sulfur and selenium under anaerobic conditions by sulfate-reducing bacterial biofilms. Appl. Environ. Microbiol. 69 (12), 7063–7072.

Ikonen, J., Voutilainen, M., Söderlund, M., Jokelainen, L., Siitari-Kauppi, M., Martin, A., 2016. Sorption and diffusion of selenium oxyanions in granitic rock. J. Contam. Hydrol. 192, 203–211.

Jain, R., Jordan, N., Tsushima, S., Hübner, R., Weiss, S., Lens, P.N.L., 2017. Shape change of biogenic elemental selenium nanomaterials from nanospheres to nanorods decreases their colloidal stability. Environ. Sci. Nano 4 (5), 1054–1063.

Jayaweera, G.R., Biggar, J.W., 1996. Role of redox potential in chemical transformations of selenium in soils. Soil Sci. Soc. Am. J. 60 (4), 1056–1063.

Kessi, J., Ramuz, M., Wehrli, E., Spycher, M., Bachofen, R., Bachofen, A.R., 1999. Reduction of selenite and detoxification of elemental selenium by the phototrophic bacterium Rhodospirillum rubrum. Appl. Environ. Microbiol. 65 (11), 4734–4740.

Kieliszek, M., Błazejak, S., 2013. Selenium: significance, and outlook for supplementation. Nutrition 29 (5), 713–718.

Klonowska, A., Heulin, T., Vermeglio, A., 2005. Selenite and tellurite reduction by Shewanella oneidensis. Appl. Environ. Microbiol. 71 (9), 5607–5609.

Law, G.T.W.W., Geissler, A., Boothman, C., Burke, I.T.I.T., Livens, F.R., Lloyd, J.R., Morris, K., 2010. Role of nitrate in conditioning aquifer sediments for technetium bioreduction. Environ. Sci. Technol. 44 (1), 150–155.

Lenz, M., Van Hullebusch, E.D., Farges, F., Nikitenko, S., Borca, C.N., Grolimund, D., Lens, P.N.L., 2008. Selenium speciation assessed by X-ray absorption spectroscopy of sequentially extracted anaerobic biofilms. Environ. Sci. Technol. 42 (20), 7587–7593.

Lortie, L., Gould, W.D., Rajan, S., McCready, R.G.L., Cheng, K.J., 1992. Reduction of selenate and selenite to elemental selenium by a Pseudomonas stutzeri isolate. Appl. Environ. Microbiol. 58 (12), 4042–4044.

Losi, M.E., Frankenberger, W.T., 1997. Reduction of selenium oxyanions by Enterobacter cloacae SLD1a-1: isolation and growth of the bacterium and its expulsion of selenium particles. Appl. Environ. Microbiol. 63 (8), 3079–3084.

Lovley, D.R., Phillips, E.J.P., 1987. Rapid assay for microbially reducible ferric iron in aquatic sediments. Appl. Environ. Microbiol. 53 (7), 1536–1540.

Lusa, M., Help, H., Honkanen, A.P., Knuutinen, J., Parkkonen, J., Kalasová, D., Bomberg, M., 2019. The reduction of Selenium(IV) by boreal Pseudomonas sp. strain T5-6-1 – effects on Selenium(IV) uptake in Brassica oleracea. Environ. Res. 177 (108642).

Macaulay, B.M., Boothman, C., van Dongen, B.E., Lloyd, J.R., 2020. A novel, "microbial bait" technique for capturing Fe(III)-reducing bacteria. Front. Microbiol. 11 (330), 1–15.

Marshall, T.A., Morris, K., Law, G.T.W., Mosselmans, J.F.W., Bots, P., Parry, S.A., Shaw, S., 2014. Incorporation of uranium into hematite during crystallization from ferrihydrite. Environ. Sci. Technol. 48 (7), 3724–3731.

Masscheleyn, P.H., Patrick, W.H., 1993. Biogeochemical processes affecting selenium cycling in wetlands. Environ. Toxicol. Chem. 12 (12), 2235–2243.

Masters-Waage, N.K., Morris, K., Lloyd, J.R., Shaw, S., Mosselmans, J.F.W., Boothman, C., Bots, P., Rizoulis, A., Livens, F.R., Law, G.T.W., 2017. Impacts of repeated redox cycling on technetium mobility in the environment. Environ. Sci. Technol. 51 (24), 14301–14310.

Morris, K., Law, G.T.W., Bryan, N.D., 2010. Geodisposal of higher activity wastes. In: Harrison, R., Hester, R. (Eds.), Nuclear Power and the Environment: Issues in Environmental Science and Technology, pp. 129–141.

Myneni, S.C., Tokunaga, T.K., Brown Jr., G.E., 1997. Abiotic selenium redox transformations in the presence of Fe(II, III) oxides. Science 278 (5340), 1106–1109.

Nakata, K., Nagasaki, S., Tanaka, S., Sakamoto, Y., Tanaka, T., Ogawa, H., 2004. Reduction rate of Neptunium(V) in heterogeneous solution with magnetite. Radiochim. Acta 92 (3), 145–149.

Nancharaiah, Y.V., Lens, P.N.L., 2015. Ecology and biotechnology of selenium-respiring bacteria. Microbiol. Mol. Biol. Rev. 79 (1), 61–80.

Oremland, R.S., Blum, J.S., Bindi, A.B., Dowdle, P.R., Herbel, M., Stolz, J.F., 1999. Simultaneous reduction of nitrate and selenate by cell suspensions of selenium-respiring bacteria. Appl. Environ. Microbiol. 65 (10), 4385–4392.

Oremland, R.S., Herbel, M.J., Blum, J.S., Langley, S., Beveridge, T.J., Ajayan, P.M., Sutto, T., Ellis, A.V., Curran, S., 2004. Structural and spectral features of selenium nanospheres produced by Se-respiring bacteria. Appl. Environ. Microbiol. 70 (1), 52–60.

Oremland, R.S., Hollibaugh, J.T., Maest, A.S., Presser, T.S., Miller, L.G., Culbertson, C.W., 1989. Selenate reduction to elemental selenium by anaerobic bacteria in sediments and culture: biogeochemical significance of a novel,sulfate-independent respiration. Appl. Environ. Microbiol. 55 (9), 2333–2343.

Peak, D., 2006. Adsorption mechanisms of selenium oxyanions at the aluminum oxide/water interface. J. Colloid Interface Sci. 303 (2), 337–345.

Peak, D., Sparks, D.L., 2002. Mechanisms of selenate adsorption on iron oxides and hydroxides. Environ. Sci. Technol. 36 (7), 1460–1466.

Pearce, C.I., Coker, V.S., Charnock, J.M., Pattrick, R.A.D., Mosselmans, J.F.W., Law, N., Beveridge, T.J., Lloyd, J.R., 2008. Microbial manufacture of chalcogenide-based nanoparticles via the reduction of selenite using veillonella atypica: an in situ EXAFS study. Nanotechnology 19 (155603).

Pearce, C.I., Pattrick, R.A., Law, N., Charnock, J.M., Coker, V.S., Fellowes, J.W., Oremland, R.S., Lloyd, J.R., 2009. Investigating different mechanisms for biogenic selenite transformations: Geobacter sulfurreducens, Shewanella oneidensis and Veillonella atypica. Environ. Technol. 30 (12), 1313–1326.

Ravel, B., Newville, M., 2005. ATHENA, ARTEMIS, HEPHAESTUS: data analysis for X-ray absorption spectroscopy using IFEFFIT. J. Synchrotron Radiat. 12 (4), 537–541.

Ruiz Fresneda, M.A., Delgado Martín, J., Gómez Bolívar, J., Cantos, M.V.F., Bosch-Estévez, G., Moreno, M.F.M., Merroun, M.L., 2018. PAPER green synthesis and biotransformation of amorphous Se nanospheres to trigonal 1D Se nanostructures: impact on Se mobility within the concept of radioactive waste disposal. Environ. Sci. Nano 5, 2103–2116.

Ruiz-Fresneda, M.A., Gomez-Bolivar, J., Delgado-Martin, J., del Mar Abad-Ortega, M., Guerra-Tschuschke, I., Merroun, M.L., 2019. The bioreduction of selenite under anaerobic and alkaline conditions analogous to those expected for a deep geological repository system. Molecules 24 (21).

Ruiz-Lopez, S., Foster, L., Boothman, C., Cole, N., Morris, K., Lloyd, J.R., 2020. Identification of a stable hydrogen-driven microbiome in a highly radioactive storage facility on the sellafield site. Front. Microbiol. 11 (587556), 1–15.

Ryser, A.L., Strawn, D.G., Marcus, M.A., Johnson-Maynard, J.L., Gunter, M.E., Möller, G., 2005. Micro-spectroscopic investigation of selenium-bearing minerals from the Western US phosphate resource area. Geochem. Trans. 6 (1), 1–11.

Saeki, K., Matsumoto, S., Tatsukawa, R., 1995. Selenite adsorption by manganese oxides. Soil Sci. 160 (4), 265–272.

Sandy, T., DiSante, C., 2010. Review of Available Technologies for the Removal of Selenium from Water. CH2MHill, pp. 2–223.

Scheinost, A.C., Charlet, L., 2008. Selenite reduction by mackinawite, magnetite and siderite: XAS characterization of nanosized redox products. Environ. Sci. Technol. 42 (6), 1984–1989.

Séby, F., Potin-Gautier, M., Giffaut, E., Donard, O.F.X., 1998. Assessing the speciation and the biogeochemical processes affecting the mobility of selenium from a geological repository of radioactive wastes to the biosphere. Analusis 26, 193–198.

Sellafield Ltd, 2016. Monitoring Our Environment Discharges and Environmental Monitoring. https://assets.publishing.service.gov.uk/government/uploads/system/uploads/attachment_data/file/658749/Monitoring_Environmental_Discharges_2016_FINAL.pdf.

Singleton, M.J., Woods, K.N., Conrad, M.E., DePaolo, D.J., Dresel, P.E., 2005. Tracking sources of unsaturated zone and groundwater nitrate contamination using nitrogen and oxygen stable isotopes at the Hanford Site,Washington. Environ. Sci. Technol. 39 (10), 3563–3570.

Söderlund, M., Virkanen, J., Holgersson, S., Lehto, J., 2016. Sorption and speciation of selenium in boreal forest soil. J. Environ. Radioact. 164, 220–231.

Stookey, L.L., 1970. Ferrozine-a new spectrophotometric reagent for iron. Anal. Chem. 42 (7), 779–781.

Switzer Blum, J., Burns Bindi, A., Buzzelli, J., Stolz, J.F., Oremland, R.S., 1998. Bacillus arsenicoselenatis, sp. nov., and Bacillus selenitireducens, sp. nov.: two haloalkaliphiles from Mono Lake, California that respire oxyanions of selenium and arsenic. Arch. Microbiol. 171 (1), 19–30.

Tabelin, C.B., Hashimoto, A., Igarashi, T., Yoneda, T., 2014. Leaching of boron, arsenic and selenium from sedimentary rocks: II. PH dependence, speciation and mechanisms of release. Sci. Total Environ. 473–474, 244–253.

Tamoto, S., Tabelin, C.B., Igarashi, T., Ito, M., Hiroyoshi, N., 2015. Short and long term release mechanisms of arsenic, selenium and boron from a tunnel-excavated sedimentary rock under in-situ conditions. J. Contam. Hydrol. 175–176, 60–71.

Tan, L.C., Nancharaiah, Y.V., van Hullebusch, E.D., Lens, P.N.L., 2016. Selenium: environmental significance, pollution, and biological treatment technologies. Biotechnol. Adv. 34 (5), 886–907.

Tan, Y., Wang, Y., Wang, Y., Xu, D., Huang, Y., Wang, D., Wang, G., Rensing, C., Zheng, S., 2018. Novel mechanisms of selenate and selenite reduction in the obligate aerobic bacterium comamonas testosteroni S44. J. Hazard. Mater. 359, 129–138.

Thorpe, C.L., Law, G.T.W.W., Lloyd, J.R., Williams, H.A., Atherton, N., Morris, K., 2017. Quantifying technetium and strontium bioremediation potential in flowing sediment columns. Environ. Sci. Technol. 51 (21), 12104–12113.

Thorpe, C.L., Lloyd, J.R., Law, G.T.W., Williams, H.A., Atherton, N., Cruickshank, J.H., Morris, K., 2016. Retention of 99mTc at ultra-trace levels in flowing column experiments – insights into bioreduction and biomineralization for remediation at nuclear facilities. Geomicrobiol J. 33 (3–4), 199–205.

Townsend, L.T., Shaw, S., Ofili, N.E.R., Kaltsoyannis, N., Walton, A.S., Mosselmans, J.F.W., Neill, T.S., Lloyd, J.R., Heath, S., Hibberd, R., Morris, K., 2020. Formation of a U(VI)-persulfide complex during environmentally relevant sulfidation of iron (oxyhydr)oxides. Environ. Sci. Technol. 54 (1), 129–136.

Viollier, E., Inglett, P.W., Hunter, K., Roychoudhury, A.N., Van Cappellen, P., 2000. The ferrozine method revisited: Fe(II)/Fe(III) determination in natural waters. Appl. Geochemistry 15 (6), 785–790.

Vogel, M., Fischer, S., Maffert, A., Hübner, R., Scheinost, A.C., Franzen, C., Steudtner, R., 2018. Biotransformation and detoxification of selenite by microbial biogenesis of selenium-sulfur nanoparticles. J. Hazard. Mater. 344, 749–757.

Weres, O., Jaouni, A.R., Tsao, L., 1989. The distribution, speciation and geochemical cycling of selenium in a sedimentary environment, Kesterson Reservoir, California, U.S.A. Appl. Geochem. 4 (6), 543–563.

WHO Technical Report Series, 1973. Trace Elements in Human Nutrition and Health. 532, pp. 1–360.

Wilkins, M.J., Livens, F.R., Vaughan, D.J., Beadle, I., Lloyd, J.R., 2007. The influence of microbial redox cycling on radionuclide mobility in the subsurface at a low-level radioactive waste storage site. Geobiology 5 (3), 293–301.

Wiramanaden, C.I.E., Liber, K., Pickering, I.J., 2010. Selenium speciation in whole sediment using X-ray absorption spectroscopy and micro X-ray fluorescence imaging. Environ. Sci. Technol. 44 (14), 5389–5394.

World Nuclear Association, Storage and Disposal Options for Radioactive Waste - World Nuclear Association. https://world-nuclear.org/information-library/nuclear-fuel-cycle/nuclear-waste/storage-and-disposal-of-radioactive-waste.aspx (accessed 2021-06-25).

Wright, M., Parker, D., Amrhein, C., 2003. Critical evaluation of the ability of sequential extraction procedures to quantify discrete forms of selenium in sediments and soils. Environ. Sci. Technol. 37 (20), 4709–4716.

Zehr, J.P., Oremland, R.S., 1987. Reduction of selenate to selenide by sulfate-respiring bacteria: experiments with cell suspensions and estuarine sediments. Appl. Environ. Microbiol. 53 (6), 1365–1369.

Zhang, Y., Zahir, Z.A., Frankenberger, W.T., 2004. Fate of colloidal-particulate elemental selenium in aquatic systems. J. Environ. Qual. 33 (2), 559–564.

Zoidis, E., Seremelis, I., Kontopoulos, N., Danezis, G.P., 2018. Selenium-dependent antioxidant enzymes: actions and properties of selenoproteins. Antioxidants 7 (5), 66.